Pain 83 (1999) 591–600

PAIN

www.elsevier.nl/locate/pain

Plasticity of sodium channel expression in DRG neurons in the chronic constriction injury model of neuropathic pain

Sulayman D. Dib-Hajj[a,b], Jenny Fjell[a,b,c], Theodore R. Cummins[a,b], Zheng Zheng[d], Kaj Fried[c], Robert LaMotte[d], Joel A. Black[a,b], Stephen G. Waxman[a,b,*]

[a]*Department of Neurology, Yale University School of Medicine, New Haven, CT 06510, USA*
[b]*PVA/EPVA Neuroscience Research Center and Rehabilitation Research Center, Veterans Affairs Medical Center, West Haven, CT 06516, USA*
[c]*Department of Neuroscience, Karolinska Institutet, SE-171 77 Stockholm, Sweden*
[d]*Department of Anesthesiology, Yale University School of Medicine, New Haven, CT 06510, USA*

Received 1 March 1999; received in revised form 5 May 1999; accepted 28 June 1999

Abstract

Previous studies have shown that transection of the sciatic nerve induces dramatic changes in sodium currents of axotomized dorsal root ganglion (DRG) neurons, which are paralleled by significant changes in the levels of transcripts of several sodium channels expressed in these neurons. Sodium currents that are resistant to tetrodotoxin (TTX-R) and the transcripts of two TTX-R sodium channels are significantly attenuated, while a rapidly repriming tetrodotoxin-sensitive (TTX-S) current emerges and the transcripts of α-III sodium channel, which produce a TTX-S current when expressed in oocytes, are up-regulated. We report here on changes in sodium currents and sodium channel transcripts in DRG neurons in the chronic constriction injury (CCI) model of neuropathic pain. CCI-induced changes in DRG neurons, 14 days post-surgery, mirror those of axotomy. Transcripts of NaN and SNS, two sensory neuron-specific TTX-R sodium channels, are significantly down-regulated as is the TTX-R sodium current, while transcripts of the TTX-S α-III sodium channel and a rapidly repriming TTX-S Na current are up-regulated in small diameter DRG neurons. These changes may provide at least a partial basis for the hyperexcitablity of DRG neurons that contributes to hyperalgesia in this model. © 1999 International Association for the Study of Pain. Published by Elsevier Science B.V.

Keywords: TTX-R Na current; Rapidly repriming Na current; Thermal hyperalgesia; RT-PCR; In situ hybridization

1. Introduction

Peripheral nerve injury in humans is associated with neuropathic pain that can be manifested as spontaneous pain, thermal and mechanical hyperalgesia and allodynia. A number of experimental models in the rat have been developed to investigate the mechanisms underlying neuropathic pain (Bennett and Xie, 1988; Seltzer et al., 1990; Kim and Chung, 1992; DeLeo et al., 1994; Gazelius et al., 1996; Kupers et al., 1998). The loose ligation of the sciatic nerve, also known as chronic constriction injury, CCI (Bennett and Xie, 1988), the tight ligation of partial sciatic nerve (PSL) of Seltzer et al. (1990) and the tight ligation of spinal nerves (SNL) of Kim and Chung (1992) are the most widely used models of neuropathic pain. Recently, a comparison of these three models by the same group demonstrated signs of ongoing and stimulus-dependent pain with similar time course, but with considerable variation of each component in the different models (Kim et al., 1997).

Normally, most small diameter dorsal root ganglion (DRG) neurons are electrically silent unless stimulated by noxious stimuli or by tissue or nerve damage which can render them hyperexcitable. These neurons include the small diameter unmyelinated C-type and thinly myelinated Aδ type fibers, the majority of which are nociceptive (Lawson, 1992). Injured DRG neurons demonstrate spontaneous firing, lower threshold of activation by thermal and mechanical stimuli, and repetitive firing when stimulated above threshold (Gallego et al., 1987; Gurtu and Smith, 1988). This hyperexcitability has been associated with the accumulation of voltage-gated sodium channels at the tips of injured neurons and at the neuromas (Devor et al., 1989; England et al., 1994, 1996). The increased density of sodium channels is one factor that could produce hyperexcitability of DRG neurons following injury to their axons (Matzner and Devor, 1994; Zhang et al., 1997). Alterna-

* Corresponding author. Department of Neurology, Yale School of Medicine, LCI 707, 333 Cedar Street, New Haven, CT 06510, USA. Tel.: +1-203-785-5947; fax: +1-203-785-7826.
E-mail address: stephen.waxman@yale.edu (S.G. Waxman)

0304-3959/99/$20.00
PII: S0304-3959(99)00169-4

tively, changes in the repertoire of sodium channel isoforms may lead to inappropriate firing (Cummins and Waxman, 1997; Schild and Kunze, 1997).

Significant plasticity in the expression of sodium currents and channels has been demonstrated in DRG neurons whose axons are transected. Sodium currents that are resistant to tetrodotoxin (TTX-R) are reduced in medium-sized (40–50 μm diameter) cutaneous afferent DRG (Rizzo et al., 1995) and small DRG ($<$ 25 μm diameter) neurons following axotomy (Cummins and Waxman, 1997). Transcripts of two TTX-R, sensory neuron-specific, sodium channels are significantly attenuated (Dib-Hajj et al., 1996, 1998). A rapidly repriming TTX-sensitive (TTX-S) Na current (Cummins and Waxman, 1997), and the transcripts of α-III sodium channel, which produces a TTX-S current when expressed in oocytes (Suzuki et al., 1988; Joho et al., 1990), become prominent following injury (Waxman et al., 1994; Dib-Hajj et al., 1996). The rapid recovery from inactivation of the TTX-S current that emerges in injured DRG neurons is expected to allow the injured neurons to fire repetitively at abnormally high frequencies (Cummins and Waxman, 1997). Moreover, the loss of TTX-R channels, which can generate persistent window currents at potentials between −60 and −20 mV due to the large overlap between the activation and steady-state inactivation curves, (Cummins and Waxman, 1997) would be expected to produce a hyperpolarizing shift in resting potential which could contribute to relieving resting inactivation and increasing the fraction of TTX-S channels available for activation. These changes in the neuronal complement of TTX-R and TTX-S Na currents may render the axotomized neurons hyperexcitable, thereby contributing to neuropathic pain following nerve injury.

We have used semi-quantitative RT-PCR, in situ hybridization and patch clamp recording from DRG neurons to investigate the plasticity of sodium currents and channels in the CCI model of neuropathic pain. We selected animals that demonstrated hind paw thermal hyperalgesia and focused on small (18–30 μm) diameter DRG neurons for these studies. Our results show that, in these hyperalgesic animals, CCI induces changes in the expression profile of both TTX-R and TTX-S sodium channels which mirror those seen after sciatic nerve transection.

2. Materials and methods

2.1. Surgery

Twenty-two adult, female Sprague-Dawley rats, weighing 240–260 g, were anesthetized with pentobarbital sodium (50 mg/kg ip) and the right sciatic nerve exposed at the mid-thigh level. Four chromic gut (4–0) ligatures were tied loosely around the nerve as described by Bennett and Xie (1988). The incision site was closed in layers and a bacteriostatic agent administered intramuscularly.

In a different set of animals, the sciatic nerve was transected at the mid-thigh level as described previously (Dib-Hajj et al., 1996, 1998). Briefly, Sprague-Dawley female rats were anaesthetized with ketamine (40 mg/kg) and xylazine (2.5 mg/kg), i.p. Sciatic nerves were exposed on the right side, ligated with 4–0 sutures proximal to the pyriform ligament, transected and placed in a silicon cuff to prevent regeneration (Fitzgerald et al., 1985). Fourteen days post axotomy (dpa), the rats were anesthetized, and control (contralateral) and axotomized (ipsilateral) L4/5 DRG were cultured for whole cell recording.

2.2. Behavioral studies

The Hargreaves method of monitoring hind paw withdrawal from an under-glass radiant heat stimulus was used with an apparatus that maintained the temperature of the glass constant at 30°C (Dirig et al., 1997). The stimulus intensity was set at a level that typically elicited foot withdrawal within 8–11 s in the absence of nerve injury. Each rat was tested on two successive days before surgery and again on the 12th and 13th postoperative day. The rats were sacrificed on the 14th day. On each test day, the rats were tested individually in groups of six, such that the stimulus was delivered once to the left hind paw (control) of each rat and then to the right hindpaw (CCI). The difference in latency obtained for the two feet of each rat was calculated by subtracting the latency for the left foot from that for the right. This process was then repeated two more times such that three latency differences were obtained within approximately 15 min. Additional measurements of three difference scores were then obtained during successive 15 min intervals until 27 latency differences had been obtained and a grand mean difference obtained for each rat for that day of testing.

2.3. RT-PCR Quantitation

Total cellular RNA was isolated from pooled L4-L5 DRGs of the control and CCI sides of five rats, respectively, and reverse transcription and quantitation were performed as described previously (Dib-Hajj et al., 1998). NaN and α-III primers used for RT-PCR were described previously (Dib-Hajj et al., 1996, 1998). SNS forward (5′-CAGAAGGAACAGGAGGTG-3′) and reverse (5′-GAAGCTCTTCTGCCCTGTAGT-3′) primers are complementary to sequences in the cytoplasmic loop linking domains I and II, and amplify a 512 bp fragment that corresponds to nucleotides 1476–1988 (GenBank accession number X92184). PCR conditions for the linear co-amplification of NaN/GAPDH, SNS/GAPDH from the respective cDNA template were determined empirically. GAPDH was used as an endogenous internal control to compensate for sample-to-sample, reverse transcription and PCR efficiency variability. To prevent inhibition of the amplification of NaN and SNS sequences by excess GAPDH templates, we delayed addition of GAPDH primers (Kinoshita et al., 1992) for five and

four cycles, respectively, followed by 22 cycles of co-amplification. Co-amplification of the less abundant α-III templates was performed similarly except that addition of GAPDH primers was delayed for nine cycles followed by, 19 cycles of co-amplification. Seven independent PCR reactions of NaN/GAPDH and of SNS/GAPDH were performed to determine the average change in the level of the respective transcripts in the pooled template.

GAPDH and sodium channel-specific primers were used at final concentrations of 0.75 and 3.75 μM, respectively. Control PCR with water or RNA template produced no amplification products (data not shown). Amplification conditions were: (i) denaturation at 94°C for 3 min, annealing at 60°C for 2 min and elongation at 72°C for 2 min; (ii) three–eight cycles of denaturation at 94°C for 30 s, annealing at 60°C for 1 min and elongation at 72°C for 1 min, followed by a pause at 20°C to add GAPDH primers; (iii), 19–22 cycles of denaturation at 94°C for 30 s, annealing at 60°C for 1 min and elongation at 72°C for 1 min; (iv) elongation at 72°C for 10 min.

2.4. Cell culture

Fourteen days following CCI, the rats were deeply anesthetized with xylazine/ketamine (40/2.5 mg/kg; i.p.) and decapitated. L4 and L5 ganglia from control and CCI sides were quickly removed and desheathed in sterile complete saline solution (CSS) (pH 7.2). The DRG were then enzymatically digested at 37°C for 20 min with collagenase A (1 mg/ml; Boerhinger-Mannheim, Indianapolis, IN) in CSS and for 15 min. with collagenase D (1 mg/ml; Boerhinger–Mannheim) containing papain (30 units/ml, Worthington Biochemical Corporation, Lakewood, NJ) in CSS. The DRG were gently centrifuged (100 g for 3 min) and the pellets triturated in DRG-media (DMEM:F12, 10% FCS, 100 units/ml penicillin and 0.1 mg/ml streptomycin) containing 1 mg/ml bovine-serum albumin (BSA, Fraction V, Sigma, St. Louis, MO) and 1 mg/ml trypsin inhibitor (Sigma). The cells derived from control and CCI sides were then plated on poly-ornithine/ laminin-coated glass coverslips, flooded with DRG media after 1 h and incubated at 37°C in a humidified 95% air /5% CO_2 incubator overnight.

2.5. In situ hybridization

Digoxigenin-labeled sense and antisense riboprobes recognizing NaN nucleotide sequence 1371–1751, SNS nucleotide sequence 1476–2129, and α-III nucleotide sequence 5912–6409 (Genbank numbering) were prepared by in vitro transcription. Transcript yield and integrity were determined by comparison to control DIG-labeled RNA (Boehringer Mannheim) on 2% agarose/2.2 M formaldehyde gel.

The expression of NaN, SNS and α-III mRNAs in individual neurons was determined by in situ hybridization as previously described (Black et al., 1996; Dib-Hajj et al., 1998). In short, coverslips from control and CCI DRG that were cultured for <24 h were fixed for 10 min. in 4% formaldehyde in 0.14 M Sorensons buffer (pH 7.2), washed several times with diethylpyrocarbonate (DEPC)-treated PBS and permeabilized with 0.1% Triton X-100 in PBS for 15 min. The coverslips were then rinsed with 2× SSC, prehybridized for 30 min and then hybridized at 58°C overnight using riboprobes (0.25–0.5 ng/ml) specific for the individual sodium channel isoforms. The coverslips were sequentially incubated in 4 × SSC, 2 × SSC, RNase A (20 mg/ml; Sigma; 37°C, 30 min.) and finally 0.2 × SSC at 58°C for 3 × 20 min. The coverslips were then blocked with 2% normal sheep serum and 1% BSA for 20 min and incubated with alkaline phosphatase-conjugated anti-digoxigenin F′ab fragments (1:500, Boerhinger–Mannheim) overnight at 4°C. Following multiple rinses, the hybridization signal was visualized using NBT histochemistry. The NBT reaction was monitored visually and stopped before the signal reached saturation.

2.6. Quantification and data analysis

Coverslips were examined with a Leica Aristoplan microscope and images were captured using a Dage 330T digital camera and IPlab Spectrum Image Analysis software. Microdensitometric quantification of the sodium channel hybridization signal was performed as previously described (Black et al., 1997). Briefly, optical density (OD) measurements of the neurons were obtained using the Scion Image analysis program. The brightfield gray levels were linearly ($R^2 > 0.99$) calibrated to OD using optical filters with OD = 0.1, 0.3 and 0.6. All hybridization signals measured were within the linear calibration range. Five separate cultures were analyzed in this study. Samples for analysis were obtained from each coverslip by arbitrarily scrolling the coverslip from the upper left quadrant and capturing the first twenty to fifty fields containing distinguishable neurons. The neurons in the captured images were outlined and the area and mean OD of each cell was determined. To permit pooling of data from the separate experiments, the ODs were normalized by dividing the OD of each neuron by the mean OD of the control cells, processed simultaneously in the same in situ hybridization experiment. Significance was assessed using Student's *t*-test at $P < 0.01$.

2.7. Whole-cell recordings

Sodium currents were recorded from DRG neurons in the whole-cell patch-clamp configuration, 18–30 h after dissociation and plating. In previous studies we have not observed significant differences in the sodium current densities measured at 4 and 24 h after plating. All recordings were made with an EPC-9 amplifier, a Macintosh Quadra 950 and the Pulse program (v 7.52, HEKA Electronic, Germany). Recording electrodes (0.8–2 MΩ) were fabricated from 1.65-mm capillary glass (WPI) using a Sutter P-87 puller. Cells were not considered for analysis if the

initial seal resistance was less than 1 GΩ or if they had high leakage currents (holding current > 1 nA at −80 mV) or an access resistance greater than 5 MΩ. The average access resistance was 2.5 ± 0.8 MΩ (mean ± standard deviation, $n = 126$). Voltage errors were minimized using 70–80% series resistance compensation. Linear leak subtraction and capacitance artifact cancellation were used for all recordings. Membrane currents were filtered at 2.5 KHz and sampled at 10 KHz. The pipette solution contained (in mM): 140 CsF, 2 $MgCl_2$, 1 EGTA, and 10 Na-HEPES (pH 7.3). The standard extracellular solution contained (in mM): 140 NaCl, 3 KCl, 2 $MgCl_2$, 1 $CaCl_2$, 0.1 $CdCl_2$, and 10 HEPES (pH 7.3). Cadmium was included to block calcium currents. The osmolarity of the solutions was adjusted to 310 mosM (Wescor 5550 osmometer). The liquid junction potential for these solutions was < 7 mV; data were not corrected to account for this offset. The offset potential was zeroed before patching the cells and checked after each recording for drift. All recordings were conducted at room temperature (~ 22°C).

3. Results

3.1. Behavioral studies

The combined mean latency differences on Hargreaves testing for all 22 rats for the two pre-operative days of testing was −0.07 ± 0.16 s. Starting 12 days after loose ligation of the sciatic nerve, all but three of these rats exhibited a more negative difference (shorter latency) on each post-operative test. The three rats that had more positive differences, that is, varying degrees of analgesia on the foot ipsilateral to the ligation, were euthanized and not included in subsequent experimental tests. For the remaining, 19 rats, the mean differences in latency for the two preoperative and two postoperative days of testing were −0.19 ± 0.13 and −2.58 ± 0.18 s, respectively. Thus, the latency of withdrawal on the foot ipsilateral to the injury decreased by 2.4 s in relation to the latency on the contralateral foot. This was a statistically significant decrease (paired t-test, $P < 0.001$).

3.2. RT-PCR

Amplification products of NaN, SNS and GAPDH, which was used as an endogenous internal control, migrated in the gel consistent with their predicted sizes of 392, 512 and 666 bp, respectively (Fig. 1A). Fig. 1B shows a significant reduction in both NaN and SNS amplification products in the DRG from the side of the CCI ('ipsilateral' side) 14 days post surgery (dps). RT-PCR results using CCI templates showed a decrease to about 57% and 58% of control NaN and SNS levels, respectively. Mean ratios ± SD for NaN/GAPDH products, for control and CCI DRG neurons were 0.8596 ± 0.0918 and 0.4908 ± 0.0644, respectively ($P < 0.001$); SNS/GAPDH products were 0.7583 ± 0.0630 and 0.4396 ± 0.0461, in control and CCI DRG, respectively ($P < 0.001$). Transcripts of α-III appear to be

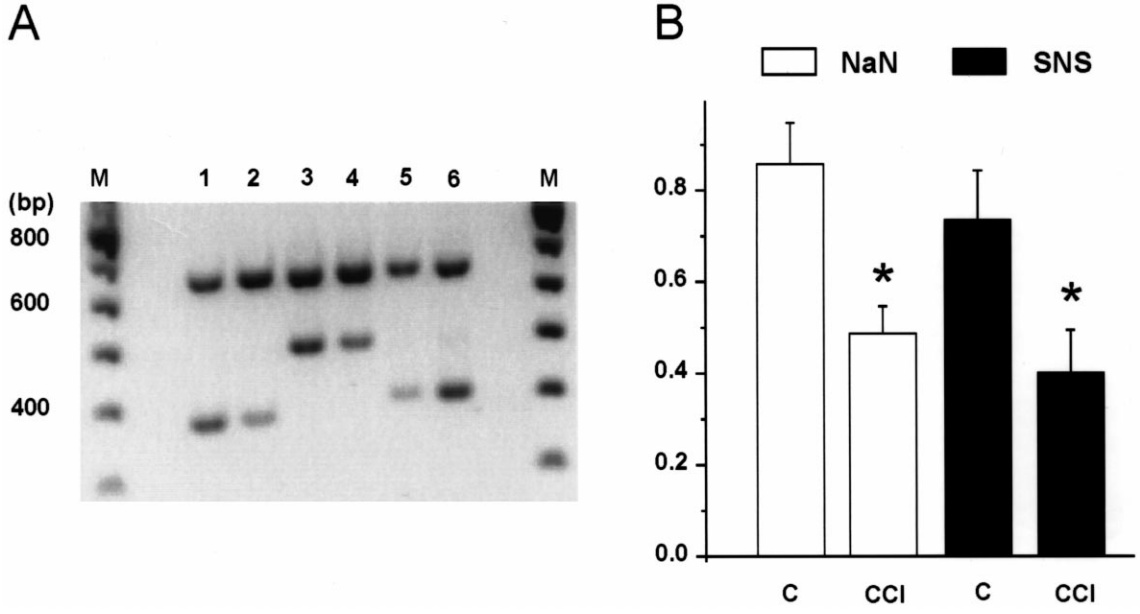

Fig. 1. Quantitation of RT-PCR products from control and CCI DRG 14 days post surgery (dps). (A) Representative gel analysis of the co-amplified NaN (392 bp), SNS (512 bp) or α-III (412 bp) and GAPDH (666 bp) products. 'M' indicates 100 bp standard (Pharmacia). Lanes 1, 3, and 5 show amplification products of GAPDH/NaN, GAPDH/SNS, and GAPDH/α-III, respectively from control neurons. Lanes 2, 4, and 6 show respective amplification products from CCI neurons. The gel picture was digitized using GelBase 7500 system (UVP, Inc.) and printed on a Fargo Primera Pro laser color printer (Fargo Electronics, Inc.) in Black and White Dye sublimation mode. (B) Average Levels of NaN and SNS amplification products normalized to GAPDH from control and CCI DRGs 14 dps. Na channel/GAPDH ratios from seven independent amplification reactions of the respective cDNA template were averaged to reduce tube-to-tube PCR variability. Data was extracted from gel analysis of PCR products as shown in (A). Error bars represent standard deviation.

up-regulated following CCI (Fig. 1A). Low levels of amplification of α-III products from control templates precluded accurate measurement of this increase.

3.3. In situ hybridization

Consistent with the RT-PCR results, most small (< 30 μm in diameter) control neurons showed strong hybridization signals for SNS and NaN riboprobes ($n = 123$, NaN; $n = 154$, SNS), while CCI neurons ($n = 116$, NaN; $n = 194$, SNS) showed weaker staining (Fig. 2, left panel). Quantification of the hybridization signals revealed that SNS and NaN signals in CCI DRG neurons were significantly reduced to 57 and 54%, respectively, of the levels in control neurons (Fig. 2, right panel; $P < 0.01$). No specific labeling was seen in control DRG neurons using α-III probes (Fig. 2E); however, moderate to strong α-III hybridization signals (Fig. 2F) were seen in about 15% (6 of 37) of CCI DRG neurons.

3.4. Electrophysiology

Whole-cell patch clamp recordings were made from small (18–30 μm diameter) DRG neurons to determine if CCI altered their sodium currents. The average diameters of the control (24.5 ± 0.4 μM; $n = 42$) and CCI (24.5 ± 0.2 μM; $n = 45$) neurons studied were similar. However, the CCI neurons appeared to generate neurites rapidly in culture, and therefore had a larger average cell capacitance (44 ± 3 pF) than did the control neurons (30 ± 2 pF). In the first set of experiments TTX was not used, and fast and slow inactivating Na currents were separated by pre-pulse inactivation (Caffrey et al., 1992; Cummins and Waxman, 1997; Elliott and Elliott, 1993; McLean et al., 1988; Rizzo et al., 1994; Roy and Narahashi, 1992).

Both fast and slow inactivating sodium currents, which we refer to as 'fast' and 'slow', respectively, were observed in the small DRG neurons. These currents were similar to those previously described in small DRG neurons (Roy and Narahashi, 1992; Caffrey et al., 1992; Elliott and Elliott, 1993; Rizzo et al., 1994; Cummins and Waxman, 1997). Almost all (95%) of the control (contralateral) cells ($n = 42$) expressed large (>200 pA/pF) fast sodium currents and the mean fast current was 26 ± 3 nA. The majority (83%) of control cells also expressed large (>200 pA/pF) slow sodium currents, with a mean slow current 22 ± 3 nA. Thus, most of control cells expressed both fast and slow sodium currents (Fig. 3A,C). In contrast, although almost all (96%) of the CCI cells ($n = 45$) expressed large fast currents (mean $= 38 \pm 4$ nA), only 18% of the CCI cells expressed large slow currents (mean $= 7 \pm 2$ nA). Thus, DRG neurons on the CCI injured side expressed predominantly fast sodium currents (Fig. 3 B,D). Due to the difference in cell capacitance, the fast current density (estimated by dividing the peak current amplitude by the cell capacitance) was similar for control and CCI neurons, but the slow current density was still much smaller for the CCI neurons (Fig. 3E).

Previously, we have shown that the fast Na currents in

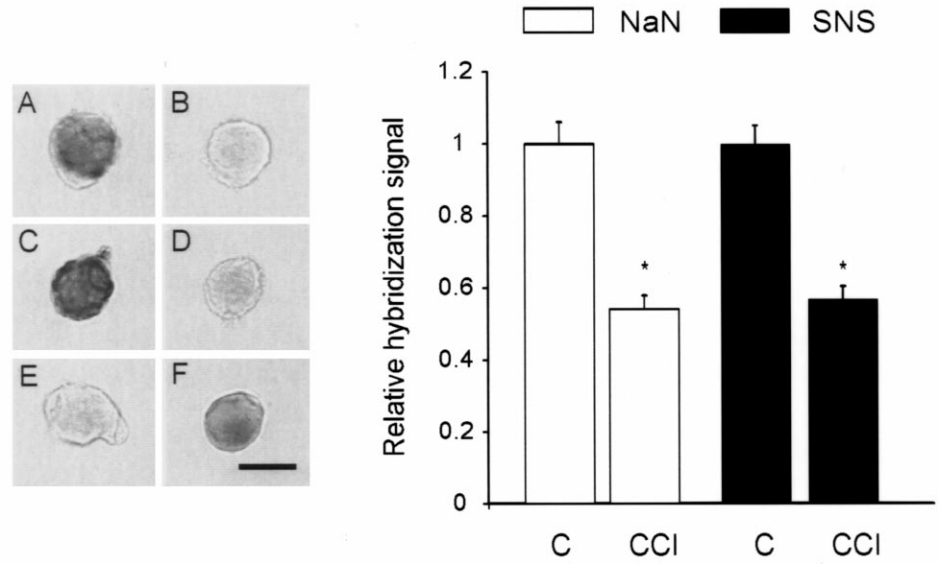

Fig. 2. In situ hybridization of small DRG neurons from control and CCI DRG 14 dps. The left panel shows cells hybridized with SNS (A,B), NaN (C,D) and α-III (E, F) probes. Whereas 61% and 59%, respectively, of small (< 30 μm) control DRG neurons show strong hybridization signal (defined as an O.D. > 0.15) using SNS (A) and NaN (C) probes, 78% and 66%, respectively, of small CCI DRG neurons show little or no staining for SNS (B) and NaN mRNA. (D). In contrast, there was an up-regulation of α-III transcripts in CCI neurons. DRG neurons from control ganglia showed no detectable hybridization signal using probes specific to α-III (E), but moderate to strong α-III hybridization signals (F) were seen in 15% of CCI neurons. Scale bar = 20 mm. The right panel shows the relative hybridization signal in small DRG neurons using SNS and NaN probes. SNS data was pooled from a total of 154 control and 194 CCI neurons from five animals. NaN data was pooled from 123 control and 116 CCI neurons from five animals. SNS and NaN levels are significantly lower ($P < 0.01$) in small CCI neurons compared to control neurons. Error bar represents standard error.

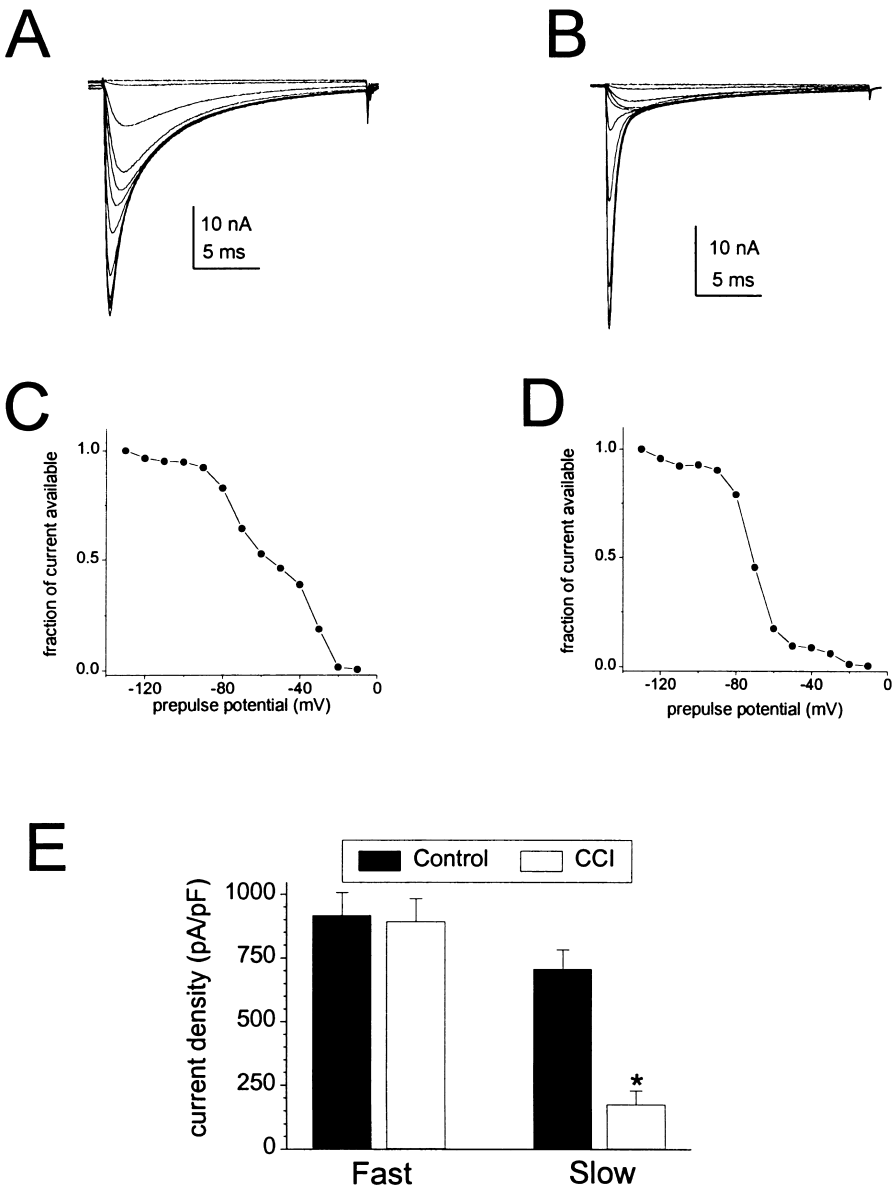

Fig. 3. Comparison of sodium currents in control and CCI DRG neurons 14 dps. A,B) Families of current traces recorded from representative neurons without TTX in the bath are shown. While the majority of the control neurons exhibited both fast and slow currents (A), the majority of CCI neurons exhibited predominantly fast currents (B). The currents were elicited by 20 ms test pulses to −10 mV after 500 ms prepulses to potentials over the range of −130 to −10 mV. (C,D) The corresponding steady-state inactivation curves for the control (C) and CCI (D) cells in (A,B) are shown. Current is plotted as a fraction of peak current. Two current components can be easily resolved in control neurons (A,C); a slowly inactivating component that has a relatively depolarized voltage-dependence of inactivation (V_h) and a fast inactivating component that has a more negative V_h. The steady-state inactivation curve for the control cell shown in A, C is bimodal, with a shoulder close to 0.5, because of the different inactivation properties of the two components. In the CCI cell (B,D), on the other hand, fast-inactivating currents predominate and the steady-state inactivation curve shows only a small shoulder close to 0.1. (E) Fast and slow peak current densities. The slow current amplitude was estimated with prepulse inactivation, where the cell was held at − 50 mV for 500 ms to inactivate the fast sodium currents. The fast current amplitude was estimated following digital subtraction of the slow component from the total current. The slow current density is significantly lower ($P < 0.0005$) in CCI neurons ($n = 45$) than in control neurons ($n = 42$). Error bars indicate SE.

axotomized neurons reprime more rapidly than the fast Na currents in control DRG neurons (Cummins and Waxman, 1997). Therefore, we examined the repriming kinetics of the fast Na currents following CCI. Repriming kinetics were measured as previously described (Cummins and Waxman, 1997; Elliott and Elliott, 1993). Cells were stepped to 0 mV for 20 ms to inactivate the Na currents, then brought back to −80 mV for increasing times before the test pulse (to 0 mV) was applied to measure the amount of current that recovered at −80 mV. The time course for recovery of the fast sodium current component was fit with a single exponential to estimate the repriming time constant. At −80 mV, the fast Na currents in CCI neurons reprimed more rapidly ($\tau = 95 \pm 14$ ms, $n = 15$) than those in control neurons

($\tau = 156 \pm 25$ ms, $n = 14$), but not as rapidly as those in axotomized neurons ($\tau = 58 \pm 6$ ms, $n = 10$). The differences between the repriming kinetics of the three groups are statistically significant ($P < 0.05$).

Recently, the presence of fast TTX-R currents has been reported in DRG neurons (Scholz et al., 1998) and in HEK cells transfected with the novel channel NaN (Tate et al., 1998). To ensure that pre-pulse inactivation did not underestimate the residual TTX-R currents in CCI neurons, we also examined sodium currents in the presence of 250 nM TTX (which blocks ~ 98% of the TTX-S current). While the majority (78%) of the control cells ($n = 18$) expressed large (> 200 pA/pF) sodium currents in the presence of TTX (mean = 28 ± 6 nA), only 33% of the CCI cells ($n = 21$) expressed similar currents (mean = 11 ± 3 nA) (Fig. 4A). The TTX-R current density distribution was roughly similar for the control and CCI neurons that expressed large TTX-R currents. In contrast to the currents studied in control neurons in the absence of TTX, where both fast and slow components of the sodium current are evident, the sodium currents studied in control neurons in the presence of 250 nM TTX were relatively homogeneous for each given cell and showed slow kinetics ($\tau_h > 2$ ms; measured at 0 mV). The residual Na current in CCI neurons also exhibited slow kinetics. As was the case for pre-pulse inactivation, CCI neurons studied in the presence of 250 nM TTX expressed significantly lower slow current densities (Fig. 4B). The percentage of CCI cells that expressed little or no sodium current in the presence of 250 nM TTX (67%) was similar to the percentage of CCI neurons that expressed only fast sodium currents in the absence of TTX (82%). When we compared other properties of the TTX-R currents in control and CCI cells, we were able to detect small differences. For example, the midpoints of activation were -15 ± 2 mV and -12 ± 3 mV and the midpoints of steady-state inactivation were -32 ± 1 mV and -29 ± 2 mV for control cells ($n = 14$) and CCI cells ($n = 8$), respectively. These differences were not, however, statistically significant.

4. Discussion

A chronic, loose constriction injury (CCI) of the sciatic nerve in rat produces behavioral signs of spontaneous pain and cutaneous hyperalgesia (Bennett and Xie, 1988). There also develops an abnormal spontaneous activity and adrenergic sensitivity of certain DRG cells with axons in the injured nerve as measured in the intact ganglion in vivo (Kajander et al., 1992; Xie et al., 1995), in vitro (Zhang et al., 1997) or in dissociated DRG cells (Petersen et al., 1996; Study and Kral, 1996). We report here on the effect of CCI of the sciatic nerve on the expression of voltage-gated sodium channels in rat DRG neurons 14 days post surgery (14 dps). All of the animals that were used in this study exhibited thermal hyperalgesia in the hindpaw ipsilateral to the injury.

Many of the axons in the CCI model undergo Wallerian degeneration, which appears to be linked to the development of neuropathic pain in this neuropathy model (Myers et al., 1993; Ramer et al., 1997). CCI nerves show greater than 80% loss of myelinated fibers and 60–80% loss of unmyelinated fibers (Carlton et al., 1991), with the spared axons intermingled with the degenerating fibers (Basbaum et al., 1991; Carlton et al., 1991). A reduction in the anterograde axonal transport of acetylcholinesterase (AchE) was delayed in the CCI model, compared with sciatic nerve crush, indicating that damage to the sciatic axons occurred secondary to the ligatures (Filliatreau et al., 1994). Furthermore, crush injury reduced AchE transport by 82% compared with a reduction of 60% after CCI, supporting the conclusion that some axons are spared in CCI (Filliatreau et al., 1994). Interestingly, in a study specifically designed to investigate changes in the gene expression of

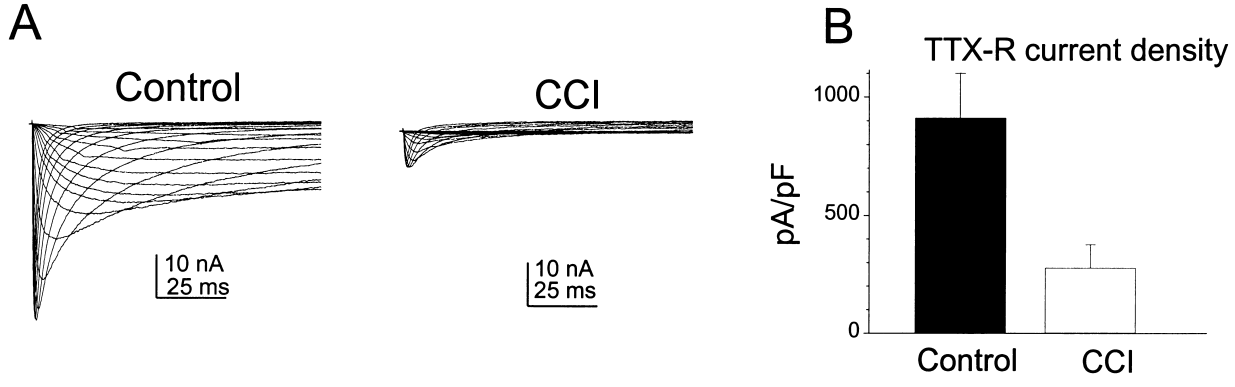

Fig. 4. Comparison of TTX-R currents in control and CCI neurons. (A) Families of voltage-activated TTX-R current traces recorded from representative control and CCI neurons with 250 nM TTX in the bath are shown. While 78% of the control neurons exhibited large (> 200 pA/pF) TTX-R currents (left; $n = 18$), only 33% of CCI cells expressed similar currents and two-thirds of the CCI cells exhibited little or no TTX-R current (right; $n = 21$). Cells were held at − 100 mV, and the currents were elicited by 200 ms test pulses ranging from − 80 to + 40 mV in 5 mV steps. (B) TTX-R peak current density from control and CCI neurons. The TTX-R current density is significantly smaller ($P < 0.005$) in CCI neurons. Error bars indicate SE.

pre-protachykinin mRNA and substance P immunoreactivity in spared neurons following CCI, it was found that these neurons demonstrate an increased level of expression of these products (Ma and Bisby, 1998). The increase in these gene products could be due to the elevated levels of NGF that result from the Wallerian degeneration of the axons distal to the ligation (Ma and Bisby, 1998).

In the present study, quantitative measurements using RT-PCR and in situ hybridization demonstrated significant reduction of transcripts for the two TTX-R channels, NaN and SNS, and the up-regulation of transcripts of the TTX-S α-III channel in small diameter DRG neurons ipsilateral to CCI. The residual NaN and SNS mRNA observed in DRG following CCI (Fig. 1) could arise from L4–L5 neurons whose axons branch before the mid-thigh site of injury, and/or from spared neurons whose axons traverse the injury site and are still in contact with their peripheral targets. The alterations in transcript levels of NaN, SNS and α-III following CCI thus mirror those following complete transection of the sciatic nerve (Cummins and Waxman, 1997; Dib-Hajj et al., 1996, 1998; Rizzo et al., 1995; Waxman et al., 1994).

Alterations in the sodium channel transcripts described above are paralleled by changes to the sodium currents in DRG neurons ipsilateral to CCI. Whole-cell patch clamp recordings from small-diameter neurons 14 dps demonstrate a significant attenuation of TTX-R currents in these neurons. This is consistent with the significant down-regulation of the transcripts for the two TTX-R Na channels, NaN and SNS. Although the TTX-S channel density did not appear to change at 14 dps, a subpopulation of the neurons from the CCI side demonstrated the appearance of a rapid-repriming Na current. These electrophysiological observations parallel our previous recordings from axotomized DRG neurons (Cummins and Waxman, 1997). However, the average rate of recovery from inactivation in CCI neurons was intermediate between that of control and axotomized neurons. This could be due to transection of only a subpopulation of axons running through the site of CCI. Alternatively, the different nature of the injury following loose ligature of the sciatic nerve, compared to axotomy, might induce a more heterogeneous mix of channels in CCI neurons, or the emergence of rapidly repriming channels may require an extra factor that is missing in CCI neurons.

Our results are consistent with the conclusion that the CCI-induced Wallerian degeneration effectively transects a significant number of the axons passing through the ligature site. Altered expression of neuropeptides in DRG neurons following CCI also mirror those following axotomy (Nahin et al., 1994). Transcripts for GAP-43, galanin, neuropeptide Y and vasointestinal peptide were up-regulated while transcripts of calcitonin gene-related peptide (CGRP) and substance P (SP) were reduced following CCI (Nahin et al., 1994). However, a recent study reported no change in TTX-R sodium currents or SNS/PN3 mRNA in small DRG neurons 14 days following CCI (Novakovic et al., 1998). These observations are difficult to reconcile with the results presented here and with previous studies on axotomized DRG neurons (Cummins and Waxman, 1997; Dib-Hajj et al., 1996, 1998; Okuse et al., 1997; Rizzo et al., 1995; Tate et al., 1998; Zhang et al., 1997). Factors that may have contributed to the disparity between our results and those of Novakovic et al. (1998) include differences in surgical techniques or behavioral testing, or could be due to the small number of CCI neurons ($n = 14$) analyzed by electrophysiology in that study. Since 30–40% of L4 and L5 neurons branch off anterior to the site of ligation and different surgical methods can result in a loss of unmyelinated axons ranging from 30 to 80% (Basbaum et al., 1991; Carlton et al., 1991), the small number of neurons studied by electrophysiology by Novakovic et al. (1998) may not have been sufficient to detect the reduction in the TTX-R Na currents in small-diameter CCI neurons.

The rats used in this study showed stimulus-evoked hyperalgesia in their paw ipsilateral to CCI. Injured nerves in this model retain spared axons (Basbaum et al., 1991; Carlton et al., 1991), which are expected to remain in contact with their peripheral targets. Injured neurons contribute to both components of neuropathic pain, ongoing and stimulus-evoked pain (Yoon et al., 1996). Small diameter CCI neurons may become hyperexcitable due to the loss of their TTX-R sodium channel complement and to the appearance of the rapidly repriming TTX-S sodium current (Cummins and Waxman, 1997). Intact nerves may produce stimulus-evoked pain by an exaggerated response to a normal stimulus due to central sensitization of dorsal horn neurons by the spontaneous activity of the injured fibers (Yoon et al., 1996). Another possible explanation for the stimulus-evoked hyperalgesia in CCI is hyperexcitability of these spared neurons, which could be partially due to changes in the expression of their sodium channels. These changes could arise from the elevated levels of neurotrophic factors, such as NGF and GDNF, in the injured nerve (Bar et al., 1998; Hammarberg et al., 1996; Heumann et al., 1987; Naveilhan et al., 1997); both NGF (Black et al., 1997; Dib-Hajj et al., 1998) and GDNF (Fjell et al., 1999) modulate the level of expression of sodium channels in DRG. This hypothesis is further supported by the finding that spared neurons over-produce pre-protachykinin and SP following CCI (Ma and Bisby, 1998). Molecular and electrophysiological studies of Na channels in identified spared neurons in CCI should be informative in determining the role of these neurons in the stimulus-evoked component of neuropathic pain which is associated with this nerve injury.

Acknowledgements

The authors thank Lynda Tyrrell and Bart Toftness for excellent technical assistance. This work was supported in part by grants from the National Multiple Sclerosis Society, the Medical Research Service and Rehabilitation Research

Service, Department of Veterans Affairs, the Paralyzed Veterans of America and Eastern Paralyzed Veterans Association (S.G.W.), PHS grants NS 14624 and NS 10174 (R. L-M), and grant 8654 from the Swedish Medical Research Council (KF). JF was supported in part by Foundation BLANCEFLOR Boncompagni-Ludovisi, nee Bildt.

References

Bar KJ, Saldanha GJ, Kennedy AJ, Facer P, Birch R, Carlstedt T, Anand P. GDNF and its receptor component Ret in injured human nerves and dorsal root ganglia. Neuroreport 1998;9:43–47.

Basbaum AI, Gautron M, Jazat F, Mayes M, Guilbaud G. The spectrum of fiber loss in a model of neuropathic pain in the rat: an electron microscopic study. Pain 1991;47:359–367.

Bennett GJ, Xie YK. A peripheral mononeuropathy in rat that produces disorders of pain sensation like those seen in man. Pain 1988;33:87–107.

Black JA, Dib-Hajj S, McNabola K, Jeste S, Rizzo MA, Kocsis JD, Waxman SG. Spinal sensory neurons express multiple sodium channel alpha-subunit mRNAs. Mol Brain Res 1996;43:117–131.

Black JA, Langworthy K, Hinson AW, Dib-Hajj SD, Waxman SG. NGF has opposing effects on Na^+ channel III and SNS gene expression in spinal sensory neurons. Neuroreport 1997;8:2331–2335.

Caffrey JM, Eng DL, Black JA, Waxman SG, Kocsis JD. Three types of sodium channels in adult rat dorsal root ganglion neurons. Brain Res 1992;592:283–297.

Carlton SM, Dougherty PM, Pover CM, Coggeshall RE. Neuroma formation and numbers of axons in a rat model of experimental peripheral neuropathy. Neurosci Letts 1991;131:88–92.

Cummins TR, Waxman SG. Downregulation of Tetrodotoxin-resistant sodium currents and upregulation of a rapidly repriming Tetrodotoxin-sensitive sodium current in small spinal sensory neurons after nerve injury. J Neurosci 1997;17:3503–3514.

DeLeo JA, Coombs DW, Willenbring S, Colburn RW, Fromm C, Wagner R, Twitchell BB. Characterization of a neuropathic pain model: sciatic cryoneurolysis in the rat. Pain 1994;56:9–16.

Devor M, Keller CH, Deerinck CJ, Levinson SR, Ellisman MH. Na^+ channel accumulation on axolemma of afferent endings in nerve end neuromas in Apteronotus. Neurosci Letts 1989;102:149–154.

Dib-Hajj S, Black JA, Felts P, Waxman SG. Down-regulation of transcripts for Na channel alpha-SNS in spinal sensory neurons following axotomy. Proc Natl Acad Sci (USA) 1996;93:14950–14954.

Dib-Hajj SD, Black JA, Cummins TR, Kenney AM, Kocsis JD, Waxman SG. Rescue of alpha-SNS sodium channel expression in small dorsal root ganglion neurons following axotomy by in vivo administration of nerve growth factor. J Neurophysiol 1998a;79:2668–2676.

Dib-Hajj SD, Tyrrell L, Black JA, Waxman SG. NaN, a novel voltage-gated Na channel, is expressed preferentially in peripheral sensory neurons and down-regulated after axotomy. Proc Natl Acad Sci (USA) 1998b;95:8963–8968.

Dirig DM, Salami A, Rathbun ML, Ozaki GT, Yaksh TL. Characterization of variables defining hindpaw withdrawal latency evoked by radiant thermal stimuli. J Neurosci Meth 1997;76:183–191.

Elliott AA, Elliott JR. Characterization of TTX-sensitive and TTX-resistant sodium currents in small cells from adult rat dorsal root ganglia. J Physiol (Lond) 1993;463:39–56.

England JD, Gamboni F, Ferguson MA, Levinson SR. Sodium channels accumulate at the tips of injured axons. Muscle and Nerve 1994;17:593–598.

England JD, Levinson SR, Shrager P. Immunocytochemical investigations of sodium channels along nodal and internodal portions of demyelinated axons. Microscopy Res and Technique 1996;34:445–451.

Filliatreau G, Attal N, Hassig R, Guilbaud G, Desmeules J, DiGiamberardino L. Time-course of nociceptive disorders induced by chronic loose ligatures of the rat sciatic nerve and changes of the acetylcholinesterase transport along the ligated nerve. Pain 1994;59:405–413.

Fitzgerald M, Wall PD, Goedert M, Emson PC. Nerve growth factor counteracts the neurophysiological and neurochemical effects of chronic sciatic nerve section. Brain Res 1985;332:131–141.

Fjell J, Cummins TR, Dib-Hajj SD, Fried K, Black JA, Waxman SG. Differential role of GDNF and NGF in the maintenance of two TTX-resistant sodium channels in adult DRG neurons. Mol Brain Res 1999;67:267–282.

Gallego R, Ivorra I, Morales A. Effects of central or peripheral axotomy on membrane properties of sensory neurones in the petrosal ganglion of the cat. J Physiol (Lond) 1987;391:39–56.

Gazelius B, Cui JG, Svensson M, Meyerson B, Linderoth B. Photochemically induced ischaemic lesion of the rat sciatic nerve. A novel method providing high incidence of mononeuropathy. Neuroreport 1996;7:2619–2623.

Gurtu S, Smith PA. Electrophysiological characteristics of hamster dorsal root ganglion cells and their response to axotomy. J Neurophysiol 1988;59:408–423.

Hammarberg H, Piehl F, Cullheim S, Fjell J, Hokfelt T, Fried K. GDNF mRNA in Schwann cells and DRG satellite cells after chronic sciatic nerve injury. Neuroreport 1996;7:857–860.

Heumann R, Korsching S, Bandtlow C, Thoenen H. Changes of nerve growth factor synthesis in non-neuronal cells in response to sciatic nerve transection. J Cell Biol 1987;104:1623–1631.

Joho RH, Moorman JR, VanDongen AM, Kirsch GE, Silberberg H, Schuster G, Brown AM. Toxin and kinetic profile of rat brain type III sodium channels expressed in Xenopus oocytes. Brain Research Mol Brain Res 1990;7:105–113.

Kajander KC, Wakisaka S, Bennett GJ. Spontaneous discharge originates in the dorsal root ganglion at the onset of a painful peripheral neuropathy in the rat. Neurosci Letts 1992;138:225–228.

Kim SH, Chung JM. An experimental model for peripheral neuropathy produced by segmental spinal nerve ligation in the rat. Pain 1992;50:355–363.

Kim KJ, Yoon YW, Chung JM. Comparison of three rodent neuropathic pain models. Exp Brain Res 1997;113:200–206.

Kinoshita T, Imamura J, Nagai H, Shimotohno K. Quantification of gene expression over a wide range by the polymerase chain reaction. Anal Biochem 1992;206:231–235.

Kupers R, Yu W, Persson JK, Xu XJ, Wiesenfeld-Hallin Z. Photochemically-induced ischemia of the rat sciatic nerve produces a dose-dependent and highly reproducible mechanical, heat and cold allodynia, and signs of spontaneous pain. Pain 1998;76:45–59.

Lawson SN. Morphological and biochemical cell types of sensory neurons, New York: Oxford University Press, 1992.

Ma W, Bisby MA. Increase of preprotachykinin mRNA and substance P immunoreactivity in spared dorsal root ganglion neurons following partial sciatic nerve injury. Eur J Neurosci 1998;10:2388–2399.

Matzner O, Devor M. Hyperexcitability at sites of nerve injury depends on voltage-sensitive Na^+ channels. J Neurophysiol 1994;72:349–359.

McLean MJ, Bennett PB, Thomas RM. Subtypes of dorsal root ganglion neurons based on different inward currents as measured by whole-cell voltage clamp. Mol and Cell Bioch 1988;80:95–107.

Myers RR, Yamamoto T, Yaksh TL, Powell HC. The role of focal nerve ischemia and Wallerian degeneration in peripheral nerve injury producing hyperesthesia. Anesthesiol 1993;78:308–316.

Nahin RL, Ren K, De Leon M, Ruda M. Primary sensory neurons exhibit altered gene expression in a rat model of neuropathic pain. Pain 1994;58:95–108.

Naveilhan P, ElShamy WM, Ernfors P. Differential regulation of mRNAs for GDNF and its receptors Ret and GDNFR alpha after sciatic nerve lesion in the mouse. Eur J Neurosci 1997;9:1450–1460.

Novakovic SD, Tzoumaka E, McGivern JG, Haraguchi M, Sangameswaran L, Gogas KR, Eglen RM, Hunter JC. Distribution of the tetrodotoxin-

resistant sodium channel PN3 in rat sensory neurons in normal and neuropathic conditions. J Neurosci 1998;18:2174–2187.

Okuse K, Chaplan SR, McMahon SB, Luo ZD, Calcutt NA, Scott BP, Akopian AN, Wood JN. Regulation of expression of the sensory neuron-specific sodium channel SNS in inflammatory and neuropathic pain. Mol and Cell Neurosci 1997;10:196–207.

Petersen M, Zhang J, Zhang JM, LaMotte RH. Abnormal spontaneous activity and responses to norepinephrine in dissociated dorsal root ganglion cells after chronic nerve constriction. Pain 1996;67:391–397.

Ramer MS, French GD, Bisby MA. Wallerian degeneration is required for both neuropathic pain and sympathetic sprouting into the DRG. Pain 1997;72:71–78.

Rizzo MA, Kocsis JD, Waxman SG. Slow sodium conductances of dorsal root ganglion neurons: intraneuronal homogeneity and interneuronal heterogeneity. J Neurophysiol 1994;72:2796–2815.

Rizzo MA, Kocsis JD, Waxman SG. Selective loss of slow and enhancement of fast Na^+ currents in cutaneous afferent dorsal root ganglion neurones following axotomy. Neurobiol Dis 1995;2:87–96.

Roy ML, Narahashi T. Differential properties of tetrodotoxin-sensitive and tetrodotoxin-resistant sodium channels in rat dorsal root ganglion neurons. J Neurosci 1992;12:2104–2111.

Schild JH, Kunze DL. Experimental and modeling study of Na^+ current heterogeneity in rat nodose neurons and its impact on neuronal discharge. J Neurophysiol 1997;78:3198–3209.

Scholz A, Appel N, Vogel W. Two types of TTX-resistant and one TTX-sensitive Na^+ channel in rat dorsal root ganglion neurons and their blockade by Halothane. Eur J Neurosci 1998;10:2547–2556.

Seltzer Z, Dubner R, Shir Y. A novel behavioral model of neuropathic pain disorders produced in rats by partial sciatic nerve injury. Pain 1990;43:205–218.

Study RE, Kral MG. Spontaneous action potential activity in isolated dorsal root ganglion neurons from rats with a painful neuropathy. Pain 1996;65:235–242.

Suzuki H, Beckh S, Kubo H, Yahagi N, Ishida H, Kayano T, Noda M, Numa S. Functional expression of cloned cDNA encoding sodium channel III. FEBS Lett 1988;228:195–200.

Tate S, Benn S, Hick C, Trezise D, John V, Mannion RJ, Costigan M, Plumpton C, Grose D, Gladwell Z, Kendall G, Dale K, Bountra C, Woolf CJ. Two sodium channels contribute to the TTX-R sodium current in primary sensory neurons. Nature Neurosci 1998;1:653–655.

Waxman SG, Kocsis JD, Black JA. Type III sodium channel mRNA is expressed in embryonic but not adult spinal sensory neurons, and is reexpressed following axotomy. J Neurophysiol 1994;72:466–470.

Xie Y, Zhang J, Petersen M, LaMotte RH. Functional changes in dorsal root ganglion cells after chronic nerve constriction in the rat. J Neurophysiol 1995;73:1811–1820.

Yoon YW, Na HS, Chung JM. Contributions of injured and intact afferents to neuropathic pain in an experimental rat model. Pain 1996;64:27–36.

Zhang JM, Donnelly DF, Song XJ, Lamotte RH. Axotomy increases the excitability of dorsal root ganglion cells with unmyelinated axons. J Neurophysiol 1997;78:2790–2794.

Zhang JM, Song XJ, LaMotte RH. An in vitro study of ectopic discharge generation and adrenergic sensitivity in the intact, nerve-injured rat dorsal root ganglion. Pain 1997;72:51–57.